

Diffusion Coefficient of CO₂ Molecules as Determined by ¹³C NMR in Various Carbonated Beverages

GERARD LIGER-BELAIR,^{*,†} ELISE PROST,[‡] MARYLINE PARMENTIER,[†]
PHILIPPE JEANDET,[†] AND JEAN-MARC NUZILLARD[‡]

Laboratoire d'Enologie, UPRES EA 2069, URVVC, Faculté des Sciences de Reims,
Moulin de la Housse, B.P. 1039, 51687 Reims, Cedex 2, France and Laboratoire de Pharmacognosie,
UMR 6013, CPCBAI Bât. 18, Moulin de la Housse, B.P. 1039, 51687 Reims, Cedex 2, France

In this paper, the NMR technique was used, for the first time, to accurately determine the diffusion coefficient D of CO₂-dissolved molecules in various carbonated beverages, including champagne and sparkling wines. This parameter plays an important role concerning the bubble growth during its rise through the liquid (see ref 3). The diffusion coefficient of CO₂-dissolved molecules D was compared with that deduced from the well-known Stokes–Einstein equation and found to significantly deviate from the general trend expected from Stokes–Einstein theory, i.e. $D^{SE} \propto 1/\eta$, where D^{SE} is the Stokes–Einstein diffusion coefficient and η the viscosity of the liquid medium.

KEYWORDS: Carbonated beverages; champagne; diffusion coefficient; carbon dioxide; bubble; effervescence; nuclear magnetic resonance

1. INTRODUCTION

In champagne, sparkling wines, and beers, carbon dioxide molecules in excess form together with ethanol when yeast ferment sugars. They are responsible for producing gas bubbles. In soda drinks and most of the fizzy waters, industrial carbonation is the source of effervescence.

In weakly supersaturated liquids such as carbonated beverages, bubble formation and growing require preexisting gas cavities with radii of curvature large enough to overcome the nucleation energy barrier and grow freely (1). In a glass poured with champagne, most of the bubble nucleation sites were recently found to be located on preexisting gas cavities trapped inside hollow and roughly cylindrical cellulose-fiber-made structures on the order of 100 μm long with a cavity mouth of several micrometers (2–4). After a bubble is released from its nucleation site, it grows as it makes its way to the surface. Bubble enlargement during ascent is caused by a continuous diffusion of dissolved CO₂ molecules through the bubble interface (2–6). It is worth noting that the decrease of hydrostatic pressure between a nucleation site in the bottom of the flute and the free surface is completely negligible (around 1% of the atmospheric pressure P_0). It causes the bubble volume to grow only about 1% and therefore plays no role in the bubble growth, as observed during ascent (2, 3, 5, 7).

In the case of champagne and sparkling wines, although no scientific evidence correlates the quality of a bubbly with the fineness of its bubbles, people nevertheless often make a connection between both. Therefore, in the past few years a better understanding of the numerous parameters involved in

the bubbling process has become an important topic in the champagne research area (7). In a preceding research article (see ref 3 and references therein), by using adequately chosen mass transfer equations, the growth rate k of bubbles ascending in a champagne was theoretically derived and connected with some physicochemical parameters of the liquid medium as follows (3)

$$k = \frac{dR}{dt} \approx 0.63 \frac{k_B \theta}{P_0} D^{2/3} \left(\frac{2\alpha \rho g}{9\eta} \right)^{1/3} \Delta c \quad (1)$$

where R is the bubble radius, k_B is the Boltzmann constant, θ is the absolute temperature, P_0 is the pressure into the bubble assumed to be equal to the atmospheric pressure, D is the diffusion coefficient of CO₂ molecules dissolved in the liquid medium, ρ is the liquid density, η is its dynamic viscosity, g is the gravity acceleration, α is a numerical factor close to 0.75, and Δc is the difference in CO₂ concentrations between the liquid bulk and the close vicinity of the bubble surface in equilibrium with the gaseous CO₂ into the rising bubble. Strictly speaking, the pressure inside the rising bubble is the sum of three terms: (i) the atmospheric pressure P_0 , (ii) the hydrostatic pressure ρgh , and (iii) the Laplace pressure $2\sigma/R$ originated in the bubble's curvature. h is the depth at which the bubble rises, and σ is the surface tension of the liquid medium. However, h varying from several millimeters to several centimeters, the surface tension of the carbonated beverages being on the order of 50 mN m^{-1} , and bubbles' radii varying from several tens to several hundreds of micrometers, the contribution of both hydrostatic and Laplace pressures are negligible in front of the atmospheric pressure. More details about the exact determination of eq 1 can be found in ref 3.

To now, the diffusion coefficient of CO₂ molecules in champagne and sparkling wines was unknown and therefore only

* To whom correspondence should be addressed. Phone:(33)3 26 91 86 14. Fax:(33)3 26 91 33 40. E-mail: gerard.liger-belair@univ-reims.fr.

[†] Laboratoire d'Enologie.

[‡] Laboratoire de Pharmacognosie.

approached through the well-known theoretical Stokes–Einstein equation ($D \approx k_B \theta / 6\pi\eta r$) derived by Albert Einstein in a famous article dated from 1905 (8), where r is the order of magnitude of the molecule's hydrodynamic radius. By considering eq 1, it can be noted that D plays a major role in the bubble growth rate during its rise through the liquid medium. Therefore, a better knowledge of this key parameter could maybe help us to better understand the significant differences in the bubble size observed between some champagnes and sparkling wines. Therefore, its exact determination has become a priority. In this work, the experimental diffusion coefficient of CO₂ molecules in five carbonated beverages (a high-quality champagne wine well-known for the fineness of its bubbles, a low-quality sparkling wine, a beer, a soda, and a fizzy water) was accurately determined by using the nuclear magnetic resonance (NMR) technique.

2. EXPERIMENTAL SECTION

2.1. Samples. All the carbonated beverages in question were first degassed under vacuum. Their respective dynamic viscosity was measured at 20 °C with an Ubbelohde capillary viscosimeter (type 50110/I). Two milliliters of each sample was then enriched in ¹³CO₂ by adding 38.7 mg (227 mM/L) of sodium hydrogencarbonate-¹³C, 99 atom % ¹³C (Sigma, St. Louis, MO). Samples were then re-acidified by using diluted HCl, mixed, and directly transferred into the NMR tube.

2.2. NMR Procedure. Experiments were performed at 20 °C on a Bruker DRX 500 spectrometer equipped with a Bruker diffusion probe with a resonance frequency of 500 MHz. The NMR static field stability was ensured using a concentric capillary tube filled with D₂O. Translational diffusion coefficient measurement was achieved through the bipolar pulse-longitudinal eddy currents delay (BPP-LED) nuclear magnetic resonance technique (9). Static field gradient pulses of duration δ were used in longitudinal magnetization labeling and unlabeled steps. In between, the spatial magnetization ordering is allowed to irreversibly evolve during a mixing delay Δ through the diffusion process. Eddy currents caused by gradient pulses were allowed to vanish during a 5 ms delay, after which a read pulse provided the necessary transverse magnetization. The detection of its free evolution gave rise to a time-domain signal, converted to a spectrum by Fourier transformation. The theoretical intensity of a spectral signal is described by the following Stejskal–Tanner relation (10)

$$I_{th} = I_0 \exp\left[-\gamma^2 a^2 \left(\Delta - \frac{\delta}{3}\right) D\right] \quad (2)$$

where γ is the gyromagnetic ratio of the studied nucleus, a the area of the gradient pulses (the integral of gradient strength over the gradient pulse length), and D the diffusion coefficient of the molecular species of interest (in the present case, the CO₂ molecules).

For each sample, a series of 14 gradient pulses with intensities G ranging from 2.6 to 39.0 G·cm⁻¹ was applied, with $\delta = 8$ ms. Each gradient pulse was shaped as a sine arch to avoid rapid commutation artifacts. Reported G values are indeed those reached in the middle (maximum) of the pulse. The squared G values were evenly spaced, according to the standard procedure. Diffusion time Δ was set to 100 ms. For each gradient value, 24 transient time domain signals were co-added to obtain an acceptable signal-to-noise ratio. The interacquisition delay was set to 20 s, a value close to the longitudinal relaxation time that was determined by the inversion recovery technique. The overall acquisition time was 2 h per sample. After Fourier transformation, the spectral peak of CO₂ was integrated to produce the experimental spectral intensities I_{exp} . The 14 spectra resulting from the 14 gradient pulses are superimposed and displayed in **Figure 1**.

Diffusion coefficient calculation involved a Levenberg–Marquard minimization of the least-squares residue of the linear fit of I_{exp} versus I_{th} computed with $I_0 = 1$. All delays being constant, the residue obtained from the 14 experimental and theoretical intensities was expressed as a function of D only. This procedure reduces the number of nonlinearly fitted parameters from two (D and I_0) to only one (D). All measurements were carried out at 20 °C. Gradient strength calibration was achieved

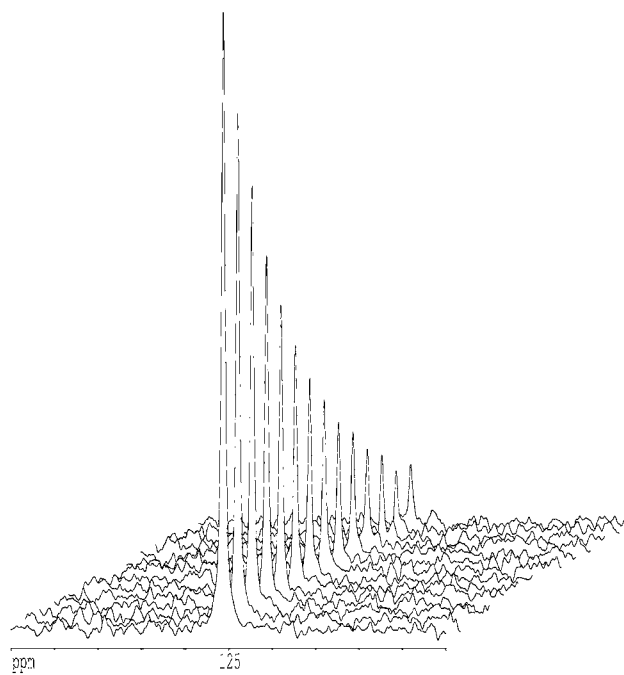


Figure 1. Evolution of the CO₂ NMR response upon variation of gradient field strength from low values (front) to high values (back).

Table 1. Dynamic Viscosity, η , of the Five Beverages and Experimental Diffusion Coefficient, D_{exp} , of Carbon Dioxide Molecules in the Five Various Sparkling Beverages

sample	η (10^{-3} kg·m ⁻¹ ·s ⁻¹)	D_{exp} (10^{-9} m ² ·s ⁻¹)
champagne wine	1.48 ± 0.02	1.41
sparkling wine	1.49 ± 0.02	1.41
beer	1.57 ± 0.03	1.44
soda	1.25 ± 0.03	1.35
fizzy water	0.96 ± 0.02	1.85

at this temperature, so that the experimental self-diffusion coefficient D value for D₂O was 1.68·10⁻⁹ m² s⁻¹ at 20 °C, as reported by Holz and Weingärtner (11).

3. RESULTS AND DISCUSSION

The five D_{exp} values of the five studied samples are reported in **Table 1** together with their respective dynamic viscosity. It can be noted from **Table 1** that the diffusion coefficient of CO₂ molecules is exactly the same in the champagne wine and in the sparkling wine. Consequently, we are logically tempted to conclude that the significant differences in the bubble size between these two “bubbly” cannot be explained from differences in their respective diffusion coefficient of CO₂ molecules. As a result, it seems that other hypotheses are to be found to explain these differences. We propose two major leads for our future investigations on the bubble growth. First, differences in the bubble size from one bubbly to another could be explained from differences in CO₂ concentrations between them (Δc in eq 1) or/and, second, from significant differences in the pool of surface-active macromolecules from one bubbly to another. Actually, in a liquid medium, it is well-known that surface-active macromolecules adsorb on the surface of a rising bubble (5, 6, 12–14), thus modifying its surface state and therefore the mass transfer of molecules through the bubble interface, in the present case, the transfer of CO₂-dissolved molecules from the liquid bulk to the carbon dioxide gas bubble (6, 15). Furthermore, in addition to this strictly hydrodynamic reason, insoluble surfactant layers can strongly modify the per-

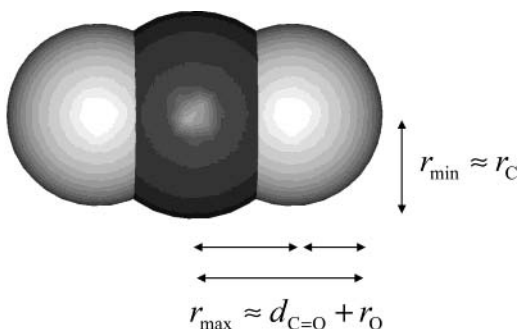


Figure 2. Schematic representation of the CO₂ molecule, and definition of r_{\max} and r_{\min} .

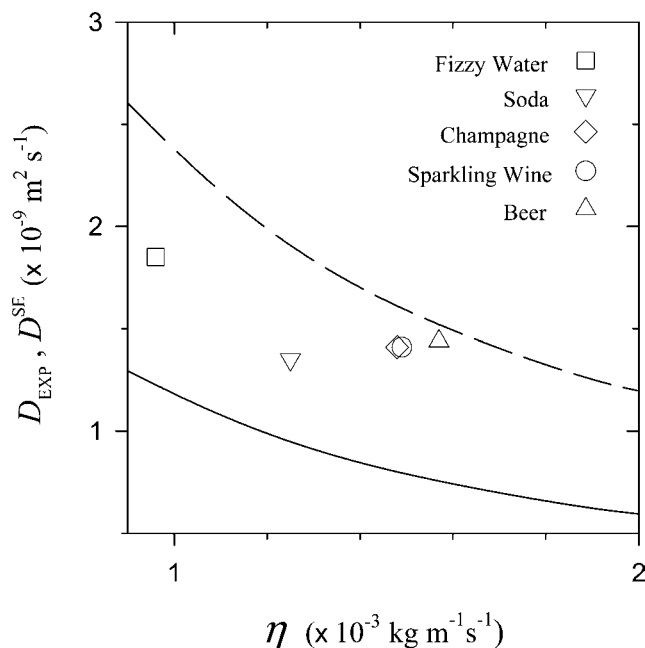


Figure 3. Experimental diffusion coefficient, D_{exp} , of carbon dioxide molecules in the five sparkling beverages plotted versus their dynamic viscosity and compared with the two limiting Stokes–Einstein equations, D_{\max}^{SE} (solid line) and D_{\min}^{SE} (long-dashed line), respectively.

meability of thin films to gases and could therefore modify the transfer of CO₂ molecules through the bubble interface (16, 17). Such considerations are nevertheless beyond the scope of this communication but will be closely examined in a near future.

We were also tempted to compare the D_{exp} values obtained by ¹³C NMR with that deduced from the Stokes–Einstein equation ($D \approx k_{\text{B}}\theta/6\pi\eta r$). It should be noted that the latter equation results from a balance between the thermal energy (the “Brownian” kinetic energy) and the viscous drag exerted by molecules close to each others. This equation considers the molecule in question as a rigid sphere, which experiences from molecules around, a Stokes’ like drag coefficient along its random walk through the solution (18). Actually, since the CO₂ molecule is far from spherical, its real hydrodynamic radius r is expected to be comprised between the two limiting values, r_{\max} and r_{\min} , as schematized in Figure 2. r_{\max} is approximated by adding the length of the C=O bond (≈ 0.116 nm) with the radius of the oxygen atom (≈ 0.065 nm), and r_{\min} is approximated by the radius of the central carbon atom (≈ 0.091 nm). In Figure 3, the five D_{exp} values of the five investigated beverages are plotted versus their respective dynamic viscosity and compared with the two limiting laws, D_{\max}^{SE} and D_{\min}^{SE} , deduced from the Stokes–Einstein equation by use of r_{\max} and

r_{\min} , respectively. As could have been logically expected, the five D_{exp} values are comprised between D_{\max}^{SE} and D_{\min}^{SE} .

It is worth noting from Figure 3 that, contrary to the general trend expected from Stokes–Einstein theory ($D^{\text{SE}} \propto 1/\eta$), the diffusion coefficient of CO₂ molecules is higher in the champagne, sparkling wine, and beer than that in the soda, their respective viscosity being nevertheless higher than that of the soda. Quite obviously, the only viscous effects cannot explain the differences of the CO₂ molecule’s mobility between the different carbonated beverages, as observed in our experiments. Interactions between the CO₂ molecule and the other species around should be investigated at a molecular scale. There may be a significant effect of dissolved salts, carbohydrates, mineral ions, etc., that could affect the colligative properties of the test matrix and thus the mobility of CO₂ molecules. The recent improvements in molecular dynamic simulation studies could help us in better understanding that kind of behavior unpredictable with the Stokes–Einstein approximation. Simulations are to be conducted along these lines.

ACKNOWLEDGMENT

Thanks are due to the Europol’Agro institute and to the “Association Recherche Oenologie Champagne Université” for financial support, to Gautier Moroy for a valuable discussion, and to Champagne Moët & Chandon and Pommery for their collaborative efforts.

LITERATURE CITED

- (1) Jones, S. F.; Evans, G. M.; Galvin, K. P. Bubbles nucleation from gas cavities: A review. *Adv. Colloid Interface Sci.* **1999**, *80*, 27–50.
- (2) Liger-Belair, G. Physicochemical approach to the effervescence in Champagne wines. *Ann. Phys. (Paris)* **2002**, *27* (4), 1–106.
- (3) Liger-Belair, G.; Vignes-Adler, M.; Voisin, C.; Robillard, B.; Jeandet, P. Kinetics of gas discharging in Champagne wines: The role of nucleation sites. *Langmuir* **2002**, *18*, 1294–1301.
- (4) Liger-Belair, G.; Marchal, R.; Jeandet, P. Close-ups on bubble nucleation in a glass of champagne. *Am. J. Enol. Vitic.* **2002**, *53*, 151–153.
- (5) Liger-Belair, G.; Marchal, R.; Robillard, B.; Dambrouck, T.; Maujean, A.; Vignes-Adler, M.; Jeandet, P. On the velocity of expanding spherical gas bubbles rising in-line in supersaturated hydroalcoholic solution: Application to bubble trains in carbonated beverages. *Langmuir* **2000**, *16*, 1889–1895.
- (6) Liger-Belair, G.; Jeandet, P. More on the surface state of expanding champagne bubbles rising at intermediate Reynolds and high Peclet numbers. *Langmuir* **2003**, *19*, 801–808.
- (7) Liger-Belair, G. The science of bubbly. *Sci. Am.* **2003**, *288* (1), 68–73.
- (8) Einstein, A. Über die von der molekularkinetischen Theorie der Wärme geforderte Bewegung von in ruhenden Flüssigkeiten suspendierten Teilchen. *Ann. Phys. (Leipzig)* **1905**, *17*, 549. Reproduced in *Investigations on the Theory of the Brownian Movement*; Dover Publications: New York, 1956.
- (9) Wu, D.; Chen, A.; Johnson, C. S. An improved diffusion-ordered spectroscopy experiment incorporating bipolar-gradient pulses. *J. Magn. Reson. A.* **1995**, *115*, 260–264.
- (10) Stejskal, E. O.; Tanner, J. E. Spin diffusion measurements: Spin-echoes in the presence of a time-dependent field gradient. *J. Chem. Phys.* **1965**, *42*, 288–292.
- (11) Holz, M.; Weingärtner, H. Calibration in accurate spin-echo diffusion measurements using ¹H and less-common nuclei. *J. Magn. Reson.* **1991**, *92*, 115–125.
- (12) Ybert, C.; di Meglio, J.-M. Ascending air-bubbles in protein solutions. *Eur. Phys. J. B* **1998**, *4*, 313–319.
- (13) Ybert, C. Stabilisation des mousses aqueuses par des protéines, Ph.D. Thesis, Université Louis Pasteur, Strasbourg, France, 1998.

- (14) Ybert, C.; di Meglio, J.-M. Ascending air bubbles in solutions of surface-active molecules: Influence of desorption kinetics. *Eur. Phys. J. E* **2000**, *3*, 143–148.
- (15) Clift, R.; Grace, J. R.; Weber, M. E. *Bubbles, Drops and Particles*; Academic Press: New York, 1978.
- (16) Princen, H. M.; Mason, S. G. The permeability of soap films to gases. *J. Colloid Interface Sci.* **1965**, *20*, 353.
- (17) Princen, H. M.; Overbeek, J. T.; Mason, S. G. *J.* The permeability of soap films to gases: A simple mechanism of monolayer permeability. *J. Colloid Interface Sci.* **1967**, *24*, 125–130.
- (18) Stokes, G. G. On the Effect of the Internal Friction of Fluids on the Motion of Pendulums. *Trans. Camb. Philos. Soc.* **1851**, *9*, 8–106.

Received for review June 27, 2003. Revised manuscript received September 5, 2003. Accepted October 9, 2003.

JF034693P